RSC Advances

PAPER

View Article Online
View Journal | View Issue

Cite this: *RSC Adv.*, 2024, **14**, 32992

Investigating the effect of overbased sulfonates on calcium sulfonate complex grease: enhancements in physicochemical, rheological, and tribological properties

Ming Zheng,[a] Guanlin Ren, *[ab] Siyuan Wang,[a] Yulong Li[b] and Mingcai Xing[c]

Overbased sulfonate plays a crucial role in calcium sulfonate complex grease, significantly impacting the grease's performance characteristics. Herein, the calcium sulfonate complex grease was formulated using overbased calcium sulfonate (T106D) and overbased magnesium sulfonate (T107) in ratios of 1 : 2, 1 : 1, and 2 : 1, labeled as CMSCG (1 : 2), CMSCG (1 : 1), and CMSCG (2 : 1), respectively. This study examined the effects of overbased sulfonates on the physicochemical, anti-corrosion, rheological, and tribological properties of the grease. Results showed that CMSCG (1 : 2) exhibited superior physicochemical properties, with the highest dropping point (354 °C), the lowest penetration (161 (0.1 mm)), and the least oil separation (1.25%). Exposure to a salt spray environment significantly altered the grease's rheological properties. The combination of T106D and T107 enhanced the corrosion resistance of the grease, attributed to the formation of a corrosion inhibition layer. Incorporating T107 increased both the yield stress and hysteresis area of the calcium sulfonate complex grease. The CMSCG (1 : 2), CMSCG (1 : 1), and MSCG showed the high thixotropic ring area, indicating the poor thixotropy. The calcium sulfonate complex grease formulated with T107 showed the highest yield stress (558 Pa). The friction mechanism revealed that MSCG showed the optimal friction reduction properties, and CMSCG (1 : 1) demonstrated the optimal wear resistance, which are attributed to the synergistic effects of tribo-chemical films composed of CaO, $CaCO_3$, $FeSO_4$, $MgCO_3$, and iron oxide.

Received 12th June 2024
Accepted 30th August 2024

DOI: 10.1039/d4ra04307c

rsc.li/rsc-advances

1 Introduction

The service life and reliability of mechanical equipment are frequently compromised under high-temperature and heavy-load conditions, often resulting in excessive wear.[1] Calcium sulfonate complex greases (CSCG) have proven to be superior lubricants in these challenging environments owing to their exceptional mechanical stability, corrosion resistance, and high dropping points. These properties make them ideal for demanding industrial applications, such as mining, marine, and steel manufacturing.[2] Overbased sulfonates, key components of CSCG, enhance anti-wear and extreme pressure capabilities, while also improve resistance to water and oxidative degradation.[3–5] By increasing alkalinity, these sulfonates inhibit the formation of acidic substances in corrosive environments and create a protective boundary film on metal surfaces, thereby enhancing lubrication performance and protecting the metal. Furthermore, the unique properties of T106D and T107 and their potential synergistic effects in CSCG formulations have not been extensively explored. This study aims to address this gap by investigating the impact of these sulfonates on the physicochemical, rheological, anti-corrosion, and tribological properties of CSCG.

The formulation of CSCG involves complex processes including the crystal form transformation and saponification of overbased calcium sulfonate (T106D), which is known for its high-temperature tolerance, superior detergency, effective rust inhibition, and significant wear resistance. Its formulation features an amorphous calcium carbonate core enveloped by an oil-soluble alkylbenzene sulfonate surfactant, essential for its functional properties.[7] During the thickening, this core transforms into vaterite and subsequently dissolves in the solvent oil, leading to a significant increase in particle size and altering the rheological properties of the grease.[8] The high alkalinity of T106D is essential for acid neutralization,[9] and at elevated alkali values, monomolecular sulfonate transitions into multimolecular micelles, a critical factor in establishing the structure and consistency of the grease. Additionally, overbased magnesium sulfonate (T107) is primarily consists of magnesium

[a]Hunan University, State Key Laboratory of Advanced Design and Manufacture for Vehicle Body, Changsha, 410082, PR China. E-mail: renguanlin@hnu.edu.cn
[b]Institute for Applied Materials-Reliability and Microstructure IAM-ZM, MicroTribology Center μTC, Karlsruhe Institute of Technology KIT, Straße Am Forum 7, Karlsruhe, 76131, Germany
[c]School of Naval Architecture, Ocean and Civil Engineering, Shanghai Jiaotong University, Shanghai 200240, PR China

alkylbenzene sulfonate that encapsulates a core of magnesium carbonate. This composition effectively neutralizes acidic byproducts from lubricant oxidation and sulfides generated during the combustion of sulfur-containing fuels. CSCG's ability to retain up to 44% water without degradation in properties underscores its robust performance in environments prone to water washout and sun irradiation, commonly found in steel mills and mining operations.[10] The hydrophilic groups within calcium sulfonate capture and retain water molecules, significantly reducing the presence of free water. Furthermore, the polarity of the SO_3^{2-} ion in overbased sulfonates plays a crucial role in enhancing the anti-corrosive properties of the grease.[11,12]

Previous studies have shown that overbased sulfonates enhance lubricant performance by forming tribofilms.[13,14] Chinas-Castillo *et al.*[15] found that overbased sulfonates form a 10–20 nanometer boundary film in lubricated contact and the film thickness increased to 3–4 particle sizes as friction progresses. However, the deposition of colloidal particles on the surface increase the surface roughness, leading to a higher in the friction coefficient. Liu *et al.*[16] investigated the tribological behavior of amorphous and crystalline overbased calcium sulfonates (AOBCS and COBCS) as lithium-based grease additives. The results indicated that crystalline overbased calcium sulfonate (COBCS), primarily composed of calcite, significantly improves anti-wear (AW), extreme pressure (EP), and friction-reducing properties compared to amorphous overbased calcium sulfonate (AOBCS). Under high load and temperature conditions, the conversion of amorphous calcium carbonate (ACC) to calcite contributes to the formation of a protective boundary film. Cizaire *et al.*[17] analyzed the friction mechanism of overbased calcium detergent through various analytical methods (XPS, AES, XANES, ToF-SIMS). Their results showed that the results revealed significant decomposition and transformation of the overbased calcium detergent's molecular structure. The resulting tribo-film is mainly composed of crystallized calcium carbonate, which provides effective protection against wear. And overbased detergent shows better anti-wear properties under low temperature conditions compared to traditional anti-wear additives. Costello *et al.*[18] examined differences in composition and structure of the surface films formed by amorphous and crystalline calcium sulfonates during friction using XPS and AES techniques. Sulfurized olefins combined with overbased calcium sulfonates improved the anti-wear properties of the friction film. Another study by Costello[19] indicated that crystalline superbased sulfonates exhibited better extreme pressure performance than amorphous sulfonates due to the formation of iron-rich FeS. $CaCO_3$ promoted the formation of iron-rich FeS by inhibiting the sulfur oxidation, thereby improving the extreme pressure performance of lubricating oil. Palermo[20] used PM-IRRAS spectroscopy to study the formation mechanism of overbased calcium sulfonate tribofilm. The results indicated that overbased calcium sulfonate formed a boundary film with preferential orientation on the steel surface, where the sulfonate chains were perpendicular to the surface and the *c*-axis of calcium carbonate was also perpendicular to the surface. During the friction process, the sulfonate chains were expelled from the contact area and the boundary film was mainly composed of calcium carbonate crystallized into calcite. These findings are significant for understanding the action mechanism of calcium sulfonate in grease and for further optimizing the grease formulation design. Greenall *et al.* found that the new lubricant additive (OAW) can not only work synergistically with ZDDP and OBCS to improve the anti-wear performance of the lubricant, but also provide similar or even better protection than ZDDP by changing the chemical composition of the friction film formed on the surface. Under the combined action of ZDDP, OBCS and OAW, a composite friction film composed of calcium phosphate, zinc phosphate and calcium carbonate is formed on the surface, showing excellent anti-wear performance.[21] Although previous studies have demonstrated the excellent anti-friction and anti-wear properties of overbased sulfonates in lubricating oils, their use as grease thickeners has not been reported. T107 is an excellent lubricating oil detergent with the advantages of strong acid neutralization ability, low ash content, and good rust resistance. Therefore, it is crucial to study the effects of T106D and T107 as the thickener of calcium sulfonate complex grease on the corrosion resistance, rheology, and tribological properties of grease.

This study explores the synergistic effects of T106D and T107 on calcium sulfonate complex grease performance. We investigate the impact of sulfonate composition on the physicochemical, rheological, anti-corrosion, and tribological properties of the greases. Furthermore, surface and interface analysis technology is used to analyze the lubrication and corrosion resistance mechanisms of overbased sulfonates.

2 Experimental

2.1 Preparation of calcium sulfonate complex grease *via* different overbased sulfonates

$Ca(OH)_2$, 12-hydroxystearic acid, and boric acid were obtained from Cologne Chemical Co., Ltd for the synthesis of the grease. T106D and T107 were sourced from Jinzhou Shengda Chemicals Co., Ltd. The base oil (castor oil) was supplied by Xilong Chemical Co., Ltd. Fig. 1 shows the structural diagram of T106D and T107. The preparation method of calcium sulfonate complex grease with different overbased sulfonates is as follows,[22] illustrated in Fig. 2. Initially, overbased sulfonates were added to the base oil at 80 °C with continuous stirring. 2 ml Glacial acetic acid was added in the base oil to achieve crystal conversion. Subsequently, boric acid and 12-hydroxystearic acid were dissolved in the mixture as the temperature was raised to 100 °C. Next, $Ca(OH)_2$ was then added into the ongoing saponification reaction with organic acids for one hour at 120 °C. The mixture was refined at a 220 °C for 20 minutes. After refining, the colloid was cooled to room temperature using a water bath and homogenized three times using a three-roll mill. To investigate the complexing effect of overbased sulfonates, the T106D and T107 were mixed in mass ratios of 1 : 2, 1 : 1, and 2 : 1. Calcium sulfonate complex grease was also prepared using T106D and T107 individually for comparison. The calcium sulfonate complex greratios of 1 : 2, 1 : 1, 2 : 1, as

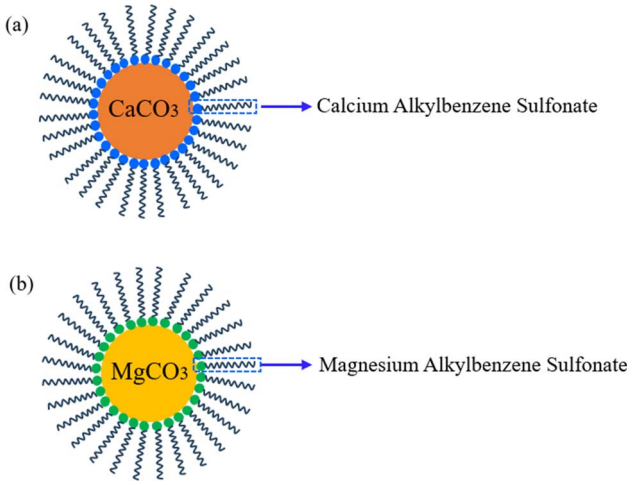

Fig. 1 The structural diagram of T106D and T107, (a) T106D, (b) T107.

well as separate T106D and T107, are abbreviated as CMSCG (1 : 2), CMSCG (1 : 1), CMSCG (2 : 1), MSCG and CSCG, respectively. The overbased sulfonates and calcium complex soap together account for 40% of the total grease. The physical properties of T106D and T107 are shown in Table 1. Table 2 presents the stoichiometry of all reactants for synthesizing the calcium sulfonate complex grease.

2.2 Physicochemical and rheological measurement

The physicochemical and rheological properties were evaluated according to the following methods.

2.2.1 Dropping point measurement. A specialized wire is used to fill the grease cup, shaping the grease into a cone. The grease cup is then placed into a designated tube, which is inserted into an aluminum block furnace maintained at a constant temperature. A thermometer is carefully inserted into the test tube, ensuring that the bottom of the thermometer does not contact the grease. When the grease first driped, the thermometer reading is recorded as the observed dropping point (t_0), and the furnace temperature is recorded as (t_1). The correction factor is calculated by dividing the difference between the observed dropping point and the furnace temperature by three. The dropping point of the grease is calculated by the formula is $T = t_0 + (t_1 - t_0)/3$. This procedure is repeated three times, and the average value is taken as the final dropping point of the grease.

2.2.2 Penetration measurement. First, the cone penetration test cup is filled with grease by a scraper. The grease is squeezed until the surface is smooth and no bubbles inside. Second, the filled test cup is then allowed to equilibrate at 25 °C for 1 hour. The test cup is positioned directly beneath the cone, and the cone tip is aligned with the grease surface. The cone is then allowed to falls freely and remains on the grease for 5 seconds. The penetration depth of the cone is measured by the instrument. Each sample is repeated three times to ensure accuracy and minimize measurement errors.

Table 1 The physical parameters of T106D and T107

Project	T106D	T107
Kinematic viscosity (100 °C, $mm^2\ s^{-1}$)	≤180	≤150
Total base number (TBN, $mg_{KOH}\ g^{-1}$)	≥395	≥390
Calcium (magnesium) content (%)	≥14	≥8.5
Flash point	≥180	≥180

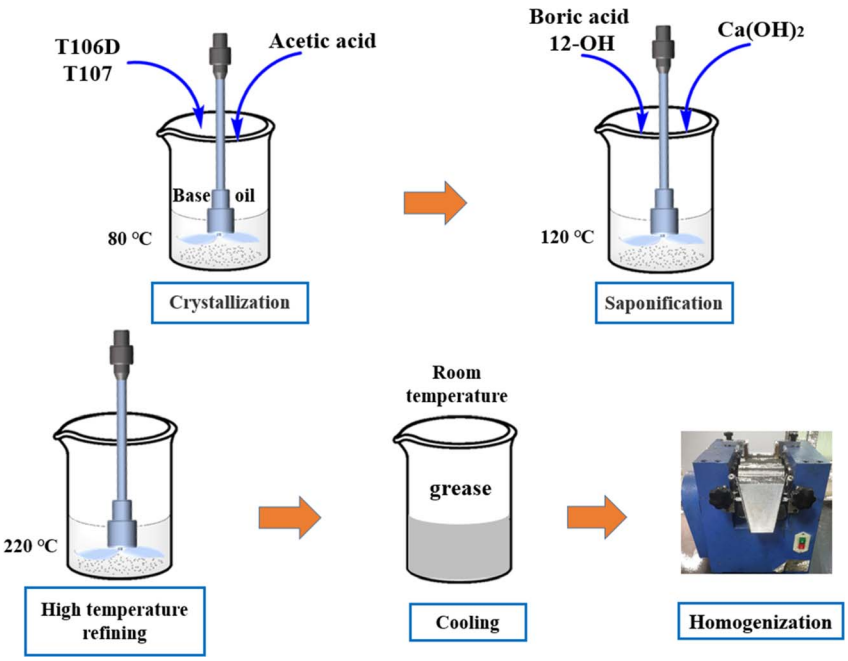

Fig. 2 The preparation process of calcium sulfonate complex grease.

Table 2 The stoichiometry of all reactants for synthesizing the calcium sulfonate complex grease

Project	Base oil (g)	T106D (g)	T107 (g)	Dodecyl hydroxystearic acid (g)	H_3BO_3 (g)	$Ca(OH)_2$ (g)
CMSCG (1 : 2)	48	5.3	10.7	8.05	2.49	5.46
CMSCG (1 : 1)	48	8	8	8.05	2.49	5.46
CMSCG (2 : 1)	48	10.7	5.3	8.05	2.49	5.46
MSCG	48	0	16	8.05	2.49	5.46
CSCG	48	16	0	8.05	2.49	5.46

2.2.3 Oil separation measurement. The weighed grease is evenly filled within the steel mesh, ensuring no gaps. The steel mesh is then placed in a standard container, which is subsequently positioned in a blast drying oven. The test is conducted at 100 °C for 24 hours. After the test, the beaker is removed and cooled to room temperature. The separated base oil collected at the bottom of the beaker is then measured using a balance, and the oil separation rate of the grease is calculated. This experiment is repeated three times to ensure the accuracy of the results.

2.2.4 Thermogravimetric measurement. The thermostability of the materials was analyzed using a Simultaneous Thermogravimetric Analyzer (STA7200), measuring changes from 25 to 600 °C at a rate of 10 °C min^{-1} under a nitrogen atmosphere.

2.2.5 Salt spray measurement. Corrosion resistance was evaluated using a salt spray test in accordance with SH/T 0081, utilizing a 5% NaCl solution at 35 °C. Mild steel (Q345) samples were coated with a 0.5 mm layer of grease to evaluate the protective efficacy of the grease. The measurement steps are as follows: the steel plate was prepared according to SH/T 0218. The grease sample was heated to a molten state, and 500 ml was measured into a beaker. The steel plate is immersed vertically into the beaker. After the temperature of the steel plate and the grease is equalized, the temperature was adjusted to change the film thickness. The steel plate was lifted at approximately 100 mm min^{-1} and hung on a rack to dry for 24 hours. The salt spray test chamber was initiated until the test conditions were met. The steel plate was placed on a support frame with the test surface facing upwards at a 15° angle to the vertical. The test sample is checked every 24 hours, and any expired or rusted test pieces were removed. Removed test pieces were first rinsed with water, then dried with hot air. The oil film was then washed with solvent oil intended for the rubber industry. Finally, the test piece was dried again with hot air. The grease thickness in this experiment was 0.5 mm, and the test cycle was 30 days, differing from SH/T 0081. Following the salt spray test, the extent of corrosion on the mild steel was examined under an optical microscope. The elemental composition of Q345 are as follows: C ≤0.20, Mn ≤1.70, Si ≤0.50, P ≤0.035, S ≤0.035.

2.2.6 Rheology measurement. Rheological properties were measured using an MCR-92 rheometer provided by AntonPaar (Shanghai) Trade Co., Ltd. The shear rate for the thixotropic loop test was set between 0.1 and 300 s^{-1}. During the test, the viscosity progression and the hysteresis area were automatically recorded. To evaluate the effect of the salt spray test on rheological properties, the thixotropic loop test was conducted under the same rheological parameters.

2.3 Tribological measurement

The tribological properties were evaluated using a four-ball tester (MRS-10A). GCr15 bearing steel balls (AISI 52100) with a diameter of 12.7 mm, hardness of HRC 59–61, and a surface roughness of $R_a = 50$ nm were used. The elemental composition of GCr15 steel is provided in Table 3. Approximately 7 g of grease was placed in the grease cup. The friction test was conducted at a rotation speed of 1200 rpm with three applied loads (294, 392, and 490 N). All measurements were carried out over a one-hour period at 25 °C. The coefficient of friction (COF) and wear scar diameter (WSD) on the three stationary balls were automatically recorded by the attached computer. To ensure accuracy, each test under the same load conditions was repeated three times.

2.4 Characterization and analysis

Field Emission Scanning Electron Microscopy (FE-SEM, IGMAHD, Carl Zeiss AG) was employed to characterize the microtopography of wear scars. Fourier Transform Infrared Spectroscopy (FTIR, Nicolet5700) was used to assess compositional changes before and after the corrosion test. The morphology and elemental composition of the wear scars were further analyzed using both FE-SEM and X-ray Photoelectron Spectroscopy (XPS, Thermo K-alpha).

3 Results and discussion

3.1 Physicochemical properties

The thickening component significantly influences the microtopography of the network and the interaction between the

Table 3 The elemental composition of GCr15 bearing steel

Elements	C	Si	Mn	P	S	Cr	Ni	Cu
Content (%)	0.9–1.5	0.15–0.35	0.25–0.45	≤0.03	≤0.025	1.35–1.65	≤0.3	≤0.3

Table 4 The physicochemical properties of the greases prepared by different overbased sulfonates

Project	Dropping point (°C)	Penetration (0.1 mm)	Oil separation (w/w %)
CMSCG (1 : 2)	354	161	1.25
CMSCG (1 : 1)	315	189	1.87
CMSCG (2 : 1)	286	227	2.03
MSCG	323	236	1.62
CSCG	275	283	1.73

thickener and base oil, thereby altering the physicochemical properties. Table 4 presents the physicochemical properties of CSCG with varying component ratio. The dropping point is a indicator of the thermal resistance of the grease. CMSCG (1 : 2) exhibits the highest dropping point at 354 °C, significantly surpassing other formulations. This indicates that a higher proportion of T107 relative to T106D enhances better thermal stability. As the proportion of T106D increases in CMSCG (2 : 1), the dropping point decreases to 286 °C, reflecting reduced thermal stability. Penetration measures the grease consistency, with lower values indicating increased firmness. CMSCG (1 : 2) again demonstrates superior performance with the lowest penetration at 161, suggesting a firmer and possibly more stable structure under mechanical stress. As the ratio of T107 decreases in CMSCG (2 : 1), the penetration value rises to 227, indicating a softer grease, which may be less effective under heavy loads. Oil separation reflects the tendency of oil to separate from the grease, which can affect lubrication performance negatively. Lower values are preferred as they indicate better stability of the grease composition. CMSCG (1 : 2) exhibits the lowest oil separation at 1.25%, suggesting it maintains its integrity better than others. Conversely, CMSCG (2 : 1) shows a higher oil separation rate of 2.03%, which may be less desirable for applications where grease longevity and consistent lubrication are critical. The synergistic effect of combining

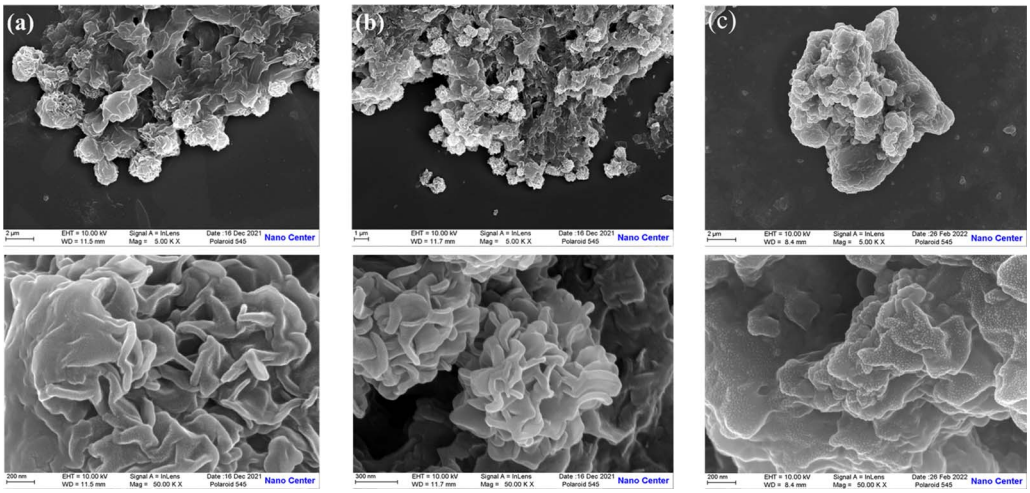

Fig. 3 The SEM images of thickener with different components, (a) CMSCG (1 : 1), (b) MSCG, (c) CSCG.

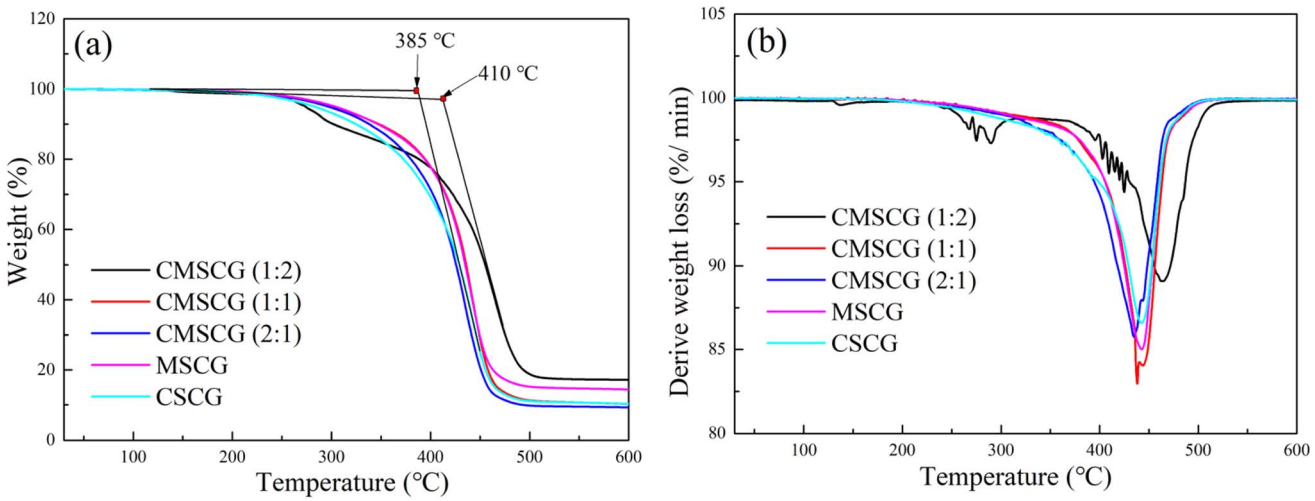

Fig. 4 The TGA and DTG curves of grease, (a) TGA, (b) DTG.

high-alkalinity calcium and magnesium sulfonates profoundly influences the physicochemical properties of the grease formulations. A higher ratio of T107 enhances thermal stability, as demonstrated by the higher dropping points. The firmness and structural integrity of the grease are better preserved with a higher proportion of T107, leading to lower penetration values. Greases with a higher proportion of calcium sulfonate also exhibit lower oil separation, signifying better stability and potential longevity in application.

Fig. 3 illustrates the microstructure of thickeners prepared with different components. The thickeners in CMSCG (1 : 1) and MSCG display flower-like microspheres with diameters ranging from 1 to 3 μm, while the particles in MSCG exhibit a tendency to accumulate. The structural evolution and crystal transformation during the preparation of calcium sulfonate complex grease are critical factors that influence its final performance. Overbased sulfonates, employed as thickeners, form a stable colloidal structure by creating a basic calcium carbonate core surrounded by an outer sulfonate shell. As the temperature increases and the reaction progresses, the crystal form of the sulfonate transitions from amorphous calcium carbonate to aragonite or calcite, which has a significant impact on the grease's performance. The incorporation of T107 enhances the formation of the flower-like structure, thereby improving the physicochemical properties of the grease. This flower-like structure exhibits excellent compatibility with the base oil, attributed to its higher specific surface area.

The thermal stability of the greases was evaluated using TGA and DTG curves, as shown in Fig. 4. CMSCG (1 : 2) exhibited a decomposition temperature of approximately 410 °C, indicating the highest thermal stability among the tested samples. In contrast, CSCG displayed a lower decomposition temperature of about 385 °C, reflecting relatively poor thermal stability. The decomposition temperatures were ranked as follows: CMSCG (1 : 2) > MSCG > CMSCG (1 : 1) > CMSCG (2 : 1) > CSCG. Greases with a higher T107 content exhibited elevated initial decomposition temperatures, attributable to T107's excellent compatibility with the base oil. The stable colloidal structure formed by CMSCG (1 : 2) contributes to its superior resistance to high temperatures.

Thermal decomposition of grease involves both physical and chemical changes as the temperature increases. Initially, the base oil separates from the thickener network and undergoes oxidation before the onset of thermal decomposition. At the initial stage of decomposition, the rate of thermal degradation is slow, primarily due to the volatilization and decomposition of the base oil. As the temperature rises, the thickener components, including overbased sulfonates and complex lithium soaps, begin to degrade. This is followed by the accelerated degradation and carbonization of the base oil. During this process, organic components decompose into small molecular gases or carbon residues. By 500 °C, the majority of grease components have decomposed, leaving primarily solid residues.

3.2 Corrosion resistance

Fig. 5 displays the SEM images of steel disk after a salt spray test. The uncoated surface exhibited severe corrosion, whereas the grease-coated disk showed minimal changes following experiment. The as-prepared calcium sulfonate complex grease exhibits excellent corrosion resistance. The synergistic effect of T106D and T107 on corrosion resistance operates through multiple mechanisms.

The FTIR spectra of the as-prepared grease, both before and after the salt spray test, are presented in Fig. 6. Peaks observed

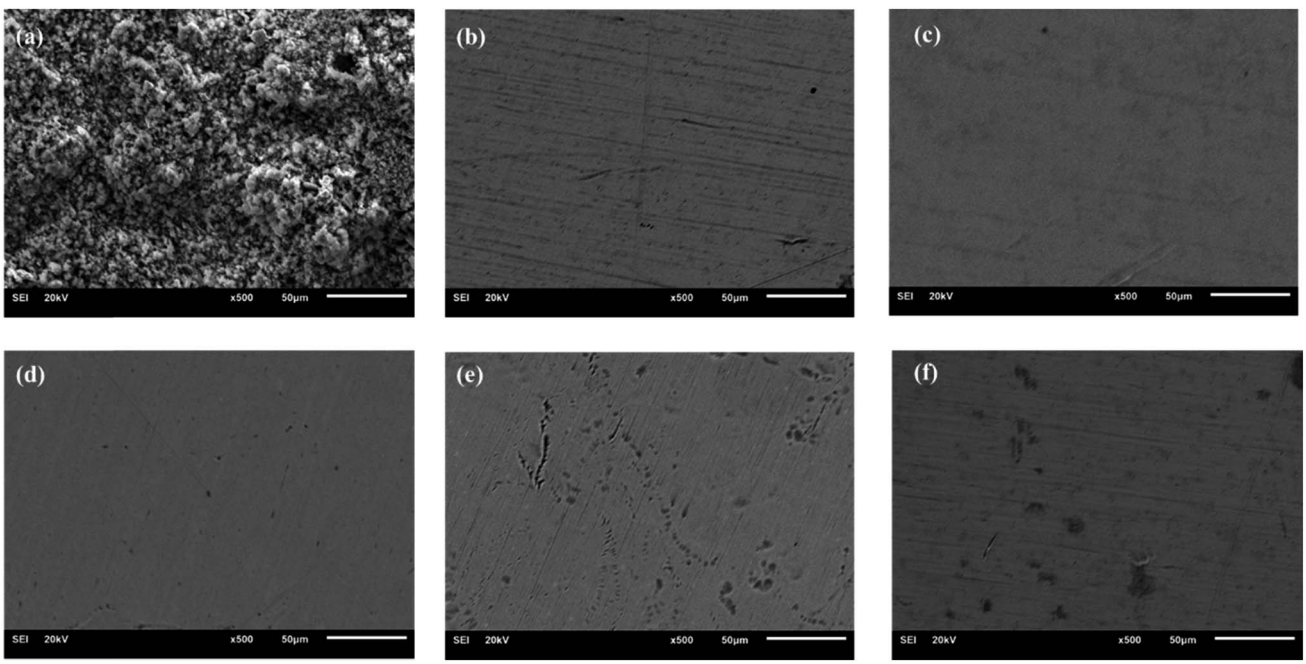

Fig. 5 The SEM of steel disks after corrosion test: (a) coating-free, (b) CMSCG (1 : 2), (c) CMSCG (1 : 1), (d) CMSCG (2 : 1), (e) MSCG, (f) CSCG.

at 1456 cm^{-1} and 1576 cm^{-1} correspond to the antisymmetric and symmetric vibrations of CO_3^{2-}, respectively.[23] The absorption at 1045 cm^{-1} is attributed to the symmetrical elongation of HSO_3^-, while the absorption at 863 cm^{-1} corresponds to the out-of-plane deformation of SO_3^-.[6] After exposure to the salt spray environment, a broad absorption band emerges around 2200 cm^{-1}, which is attributed to –OH groups or hydrogen bonding. This suggests that the grease absorbs more water under salt spray conditions, with the free water molecules contributing to the formation of hydrogen bonds. The presence of these water molecules also leads to the degradation of HSO_3^-, as demonstrated by the weakening of its characteristic absorption. High alkalinity calcium sulfonate plays a crucial role in corrosion inhibition, creating an alkaline environment that neutralizes or mitigates acidic corrosion resulting from oxidation or moisture.[24] This alkaline environment effectively slows the corrosion process on metal surfaces.[25] Additionally, high alkalinity calcium sulfonate forms a stable adsorption layer on metal surfaces, isolating the metal from corrosive agents, such as water and oxygen, thereby providing significant protection against erosion.[26] It also promotes the formation of a passivation layer, primarily composed of decomposition products such as calcium carbonate, which enhances the chemical stability of the metal surface and increases its resistance to environmental factors.[27] Furthermore, high alkalinity calcium sulfonate excels in isolating and absorbing moisture, a precess critical for reducing direct water contact with the metal surface and consequently decreasing corrosion rates.[28] It reacts with corrosive substances such as sulfides and chlorides within the grease, forming insoluble and stable compounds, which prevent these chemicals from corroding the metal surface. These collective actions confirm high alkalinity calcium sulfonate as an effective corrosion inhibitor, significantly enhancing the protective properties of grease. This enhancement extends the operational lifespan of mechanical equipment by safeguarding metal components from corrosive damage. Fig. 7 shows the photographs of steel plate before and after salt spray test and Fig. 8 illustrates the anti-corrosion mechanism of overbased sulfonates.

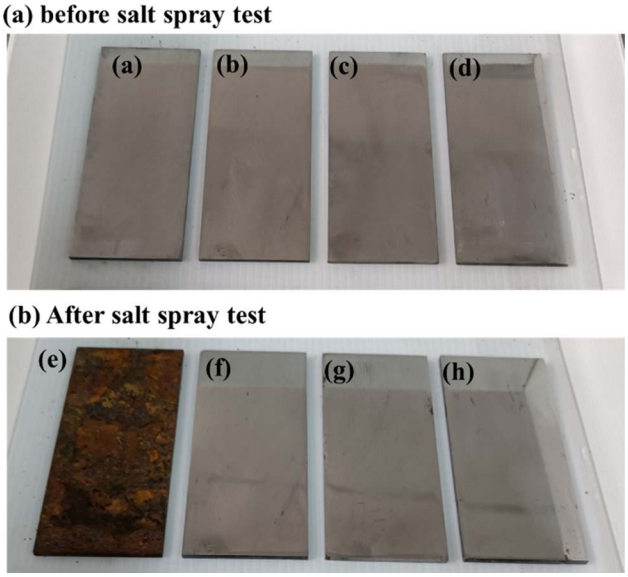

Fig. 7 The photographs of steel plate before and after salt spray test, (a and e) coating-free sample, (b and f) CMSCG (1 : 1), (c and g) MSCG, (d and h) CSCG.

3.3 Rheological properties

The influence of thickener component on the thixotropy of as-prepared grease was characterized using the thixotropic loop test, as depicted in Fig. 9. The thixotropic loops of CMSCG (1 : 2), CMSCG (1 : 1), and MSCG are notably larger than those of other greases, indicating that the higher concentration of T107 has the poorer structural recovery. And the CMSCG (2 : 1) shows the lowest thixotropic ring area (hysteresis area), indicating the CMSCG (2 : 1) has the best thixotropy. The hysteresis area reflects the structural recovery of as-prepared grease. The relative low hysteresis area indicates that the CSCG easily recovers

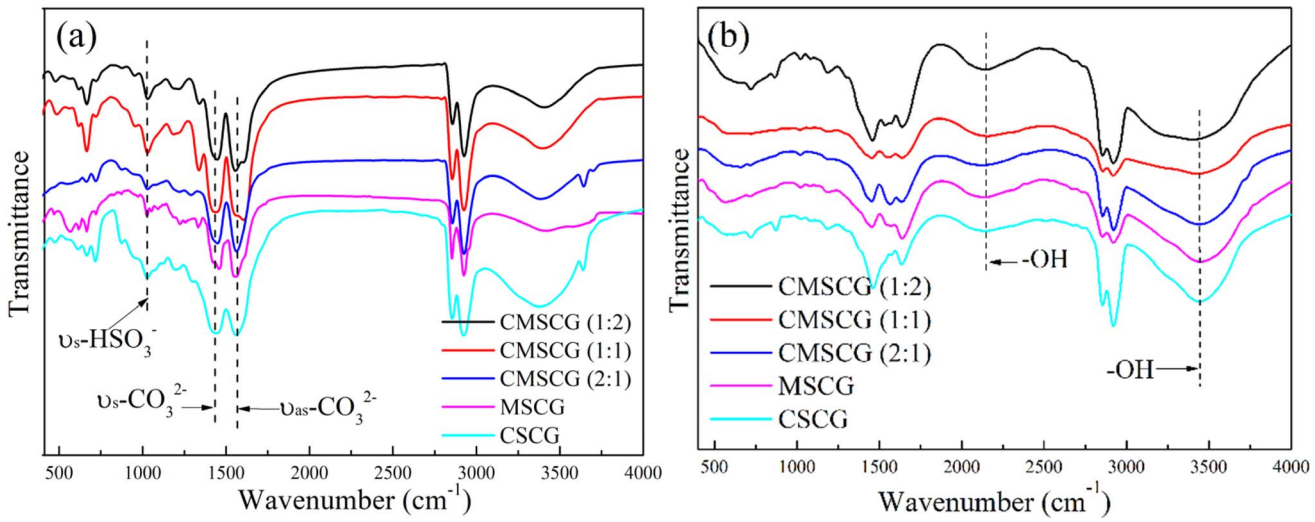

Fig. 6 The FTIR of as-prepared grease before and after salt spray test, (a) before salt spray test, (b) after salt spray test.

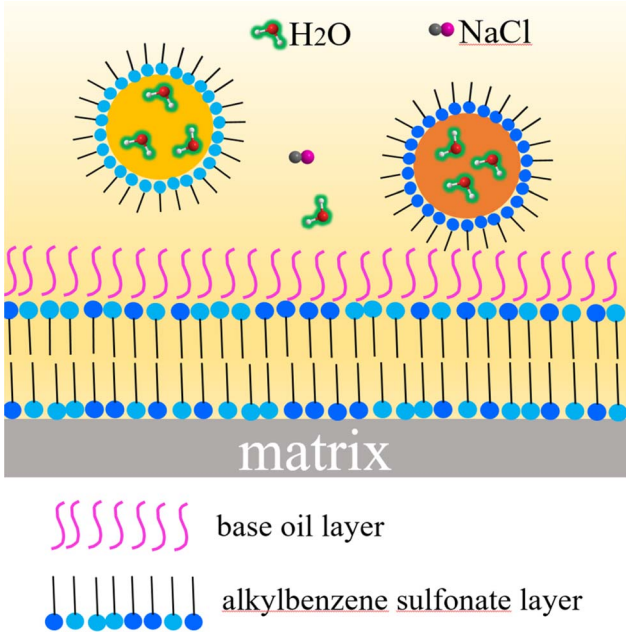

Fig. 8 The corrosion resistance mechanism of as-prepared grease.

its original structure after shear damage. The Herschel–Bulkley model (eqn (1)) is the most commonly used model to reflect the rheological properties, and it could be used to acquire grease's rheological parameters.

$$\tau = \tau_y + \phi\dot{\gamma}^n \quad (1)$$

The τ, τ_y, ϕ and n represents the shear stress, yield stress, plastic viscosity, and rheological index, respectively. Table 5 presents the relevant rheological parameters. MSCG shows the maximum yield stress, while CSCG shows the lowest yield stress. The CMSCGs with different ratio of overbased sulfonates show higher yield stress than CSCG, in which the CMSCG has the maximum yield stress. The compound of T107 and T106D increases the yield stress of CSCG, proving the flower-like spherical structure contributing to enhance the yield stress of grease. The rheological index (n) represents the mobility of grease, where the n is closer to 1, the closer the grease is to Newtonian fluid. In summary, the complex effect of T107 and T106D provides the thickener with flower-like microsphere, which reinforces the structural strength and increases the hysteresis area.

3.4 Tribological properties

The influence of overbased sulfonates on friction-wear properties was measured using a four-ball tester under three loads (294, 392 and 490 N), as depicted in Fig. 10. MSCG exhibits the lowest COF across all applied loads, indicating its superior friction reduction performance. Conversely, CSCG consistently shows the highest COF at all loads, reflecting its poor friction reduction capabilities. At 294 N, CMSCG (1 : 2) maintains the lowest friction and the CMSCG shows incrementally higher COFs as the ratio of T107 increases. The COF of CMSCG (1 : 2) is reduced by 22.8% compared to CSCG. At 392 and 490 N, MSCG achieves the lowest COF, reducing the COF by 16.4% and 12.3% compared to CSCG, respectively. Overbased sulfonates mainly affect the COF of grease in the following aspects. On the one hand, the increased shear and temperature at higher load can lead to the breakdown of the thickener structure, particularly in greases with weaker or less stable thickener systems. This structural degradation diminishes the film-forming properties of grease and increases friction. As a result, CMSCG (2 : 1) and CSCG exhibit high COF due to their lower structural strength. Except for CSCG, the COF of all other greases at 490 N are greater than those at 294 N. This further proves that high loads will destroy the stability and thickness of the lubricating film, resulting in an increase in COF. On the other hand, the microstructure of the thickener significantly influences its performance. The flower-like structure of the thickener has a stronger oil storage capacity and can release more base oil to

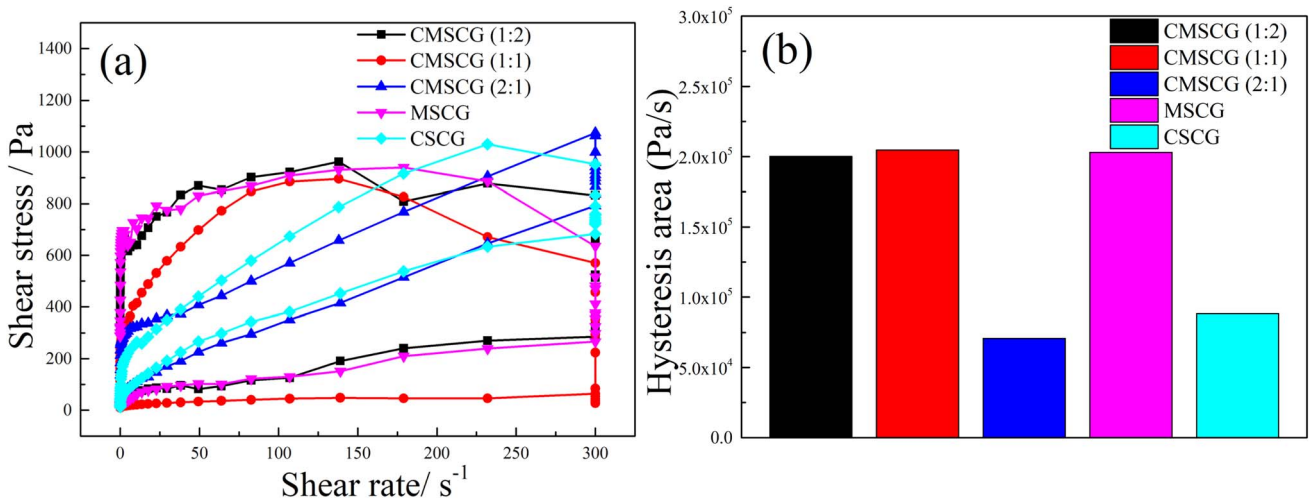

Fig. 9 The results of thixotropic ring test for as-prepared grease, (a) shear stress, (b) hysteresis area.

Table 5 The rheological parameters of the grease prepared by different overbased sulfonates

Project	τ_y, (Pa)	ϕ, (Pa s^n)	(n)
CMSCG (1 : 2)	352	206	0.22
CMSCG (1 : 1)	245	37	0.64
CMSCG (2 : 1)	280	311	0.15
MSCG	558	53	0.40
CSCG	160	14	0.68

provide lubrication when sheared, ensuring lower COF of MSCG under various loads.

For the anti-wear properties, MSCG exhibits superior performance with the smallest WSD at 294 N, reducing WSD by 30.5% compared to CSCG the CMSCG (1 : 2) shows the lowest WSD at 392 N, whereas CMSCG (1 : 1) shows the lowest WSDs and 490 N. CMSCG (1 : 2) and CMSCG (1 : 1) reduce the WSD of CSCG by 28.9% and 21.8%, respectively, indicating that the addition of T107 improved the anti-wear properties of calcium sulfonate complex grease. In summary, MSCG offers the best friction reduction property, while CMSCG (1 : 1) provides the best anti-wear property.

3.5 Tribological mechanism analysis

Fig. 11 illustrates the morphological characteristics of wear scars. CSCG exhibits the largest wear scar, while CMSCGs display smaller scars with relatively shallow furrows, indicating that the combination of T106D and T107 enhances anti-wear properties. CMSCG (2 : 1) shows ground surfaces and signs of exfoliation, characteristic of adhesive wear. In contrast, both MSCG and CSCG present deeper furrows, suggestive of abrasive wear on the worn surfaces.

To investigate the impact of thickener components on the friction mechanism, XPS analysis of worn surfaces are shown in Fig. 12. The C 1s peak, used for charge correction, is located at 284.8 eV. Oxygen-related peaks observed at 529.0, 529.5, 531.3, and 531.8 eV correspond to various iron oxides (Fe_2O_3, Fe_3O_4, Fe(OH)O) and calcium oxide (CaO).[29,30] The Fe 2p spectrum features distinct peaks at 710.1 and 710.5 eV, with a broad peak around 724.0 eV, indicating the formation of iron oxide.[31] A minor peak at 168.6 eV in the S 2p spectrum suggests the presence of iron sulfate ($FeSO_4$).[32,33] The Ca 2p spectra show peaks at 347.3 and 350.8 eV, consistent with the formation of CaO and calcium carbonate ($CaCO_3$).[34] Additionally, the Mg 1s spectrum reveals a subtle peak at 1304.0 eV, associated with

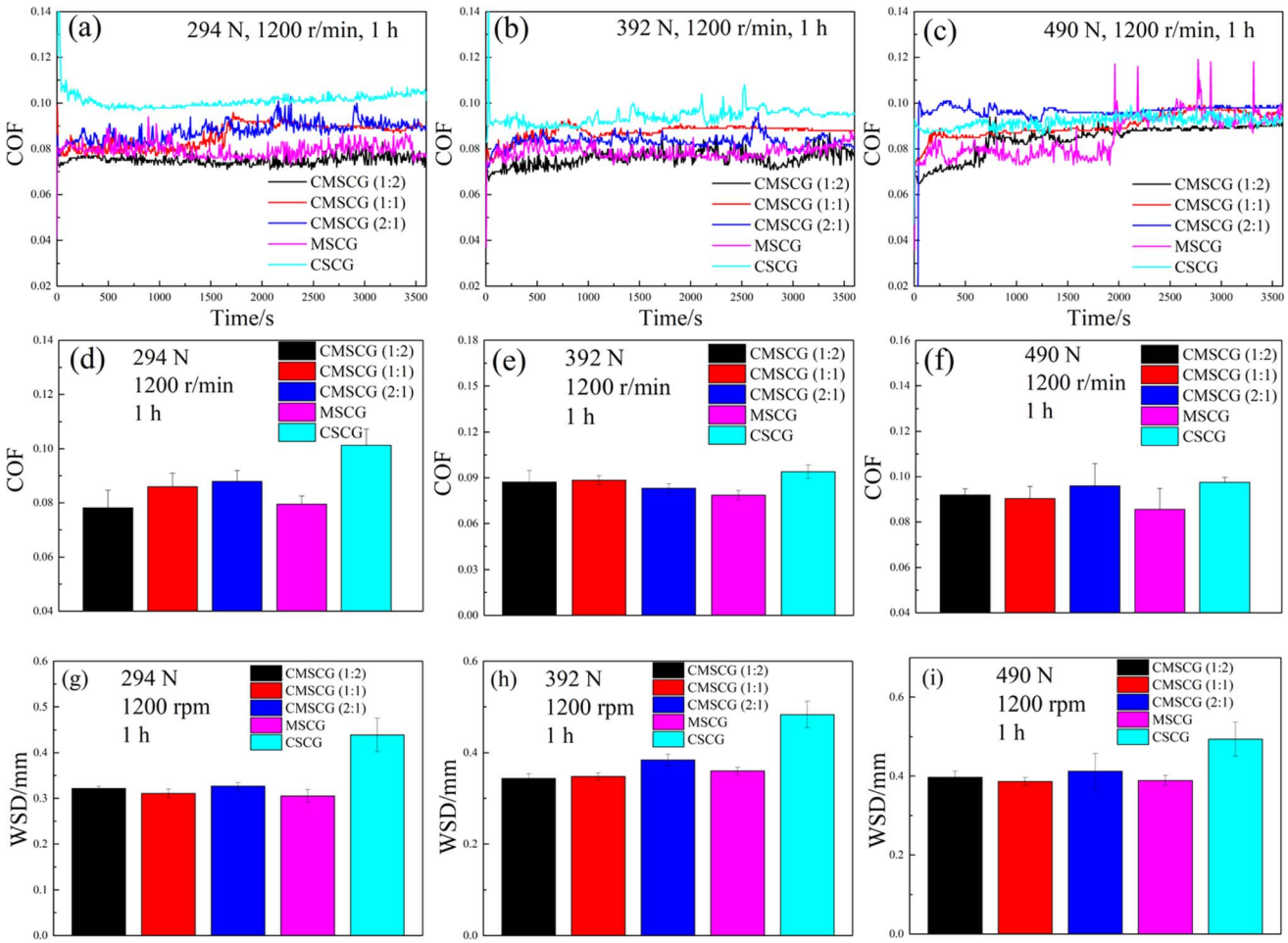

Fig. 10 Effects of overbased sulfonates on COF and WSD of calcium sulfonate complex greases, (a–c) COFs *versus* time, (d–f) average COFs of as-prepared greases, (g–i) the corresponding WSD at three different loads.

magnesium carbonate ($MgCO_3$). Under conditions of frictional heat and high stress, the thickener readily adheres to contact surfaces, contributing to the formation of a tribo-chemical film. Fe(OH)O, known for its dense and robust structure, provides exceptional wear resistance.[35,36] Although the boundary lubrication film is continually removed by abrasion, it is replenished by the thickener, ensuring a sustained protective layer on the wear surface.

The XPS spectra of MSCG and CSCG are deconvoluted to compare the differences in the chemical components of the wear scar. Fig. 13 and Table 6 shows the deconvoluted XPS spectra and corresponding FWHM and area. In the Fe 2p spectra of both greases, three distinct peaks were observed. The peak at 710.1 (710.6) eV is due to FeS, while the peak at 712.3 (713.1) eV is attributed to Fe(OH)O and Fe_2O_3. FeS is generated by the tribochemical reaction between T107 and the matrix during the friction process, and is adsorbed on the substrate surface to form a lubricating film that reduces friction.[37] The Fe $2p_{1/2}$ peaks at 724.4 and 724.8 eV are attributed to Fe_2O_3. The FWHM and peak area of the Fe $2p_{1/2}$ peak in MSCG are larger than those in CSCG, indicating that the Fe_2O_3 content in the MSCG lubricating film is higher.[38]

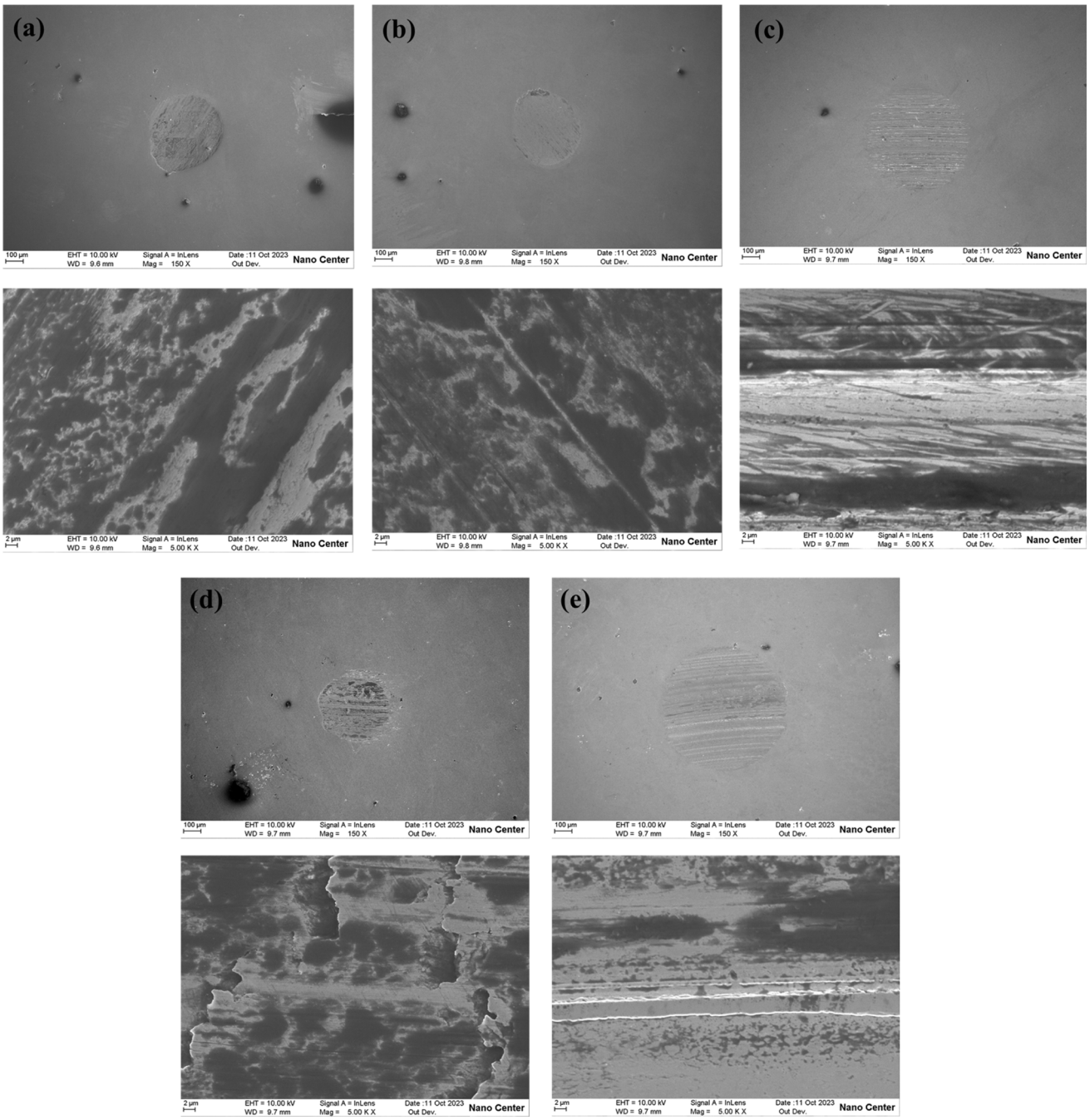

Fig. 11 The surface morphology of the wear scar at 392 N, (a) CMSCG (1 : 2), (b) CMSCG (1 : 1), (c) CMSCG (2 : 1), (d) MSCG, (e) CSCG.

The O 1s spectrum shows three peaks attributed to iron oxide and Fe(OH)O. The spectra reveal that MSCG contains more Fe(OH)O than CSCG, but less Fe_2O_3. Fe_2O_3, a product of matrix oxidation under friction, is known for its high hardness and wear resistance.[39] However, a high Fe_2O_3 content can increase the roughness of the friction surface, leading to higher friction coefficients. Thus, a lubricating film with a high Fe_2O_3 content, as seen in CSCG, results in poorer friction reduction and anti-wear performance. The S 2p spectra of the two greases are located at 168.7 and 168.8 eV, respectively. Notably, CSCG shows a peak for $CaCO_3$ at 531.4 eV, while MSCG contains more Fe(OH)O. Fe(OH)O, with its higher hardness, forms a strong and wear-resistant friction film on the surface, whereas $CaCO_3$, being relatively soft, offers poorer friction reduction and anti-wear properties. Consequently, MSCG exhibits superior tribological performance compared to CSCG. The S 2p spectra of MSCG also show peaks for $MgSO_4$ and $FeSO_4$, whereas CSCG's S 2p peak only shows $FeSO_4$. This indicates that a tribochemical reaction occurs in T107 during friction. The Ca 2p spectrum displays characteristic peaks for $CaCO_3$ and CaO, with CSCG showing stronger peaks. In summary, the high Fe(OH)O and $MgSO_4$ content in the MSCG lubricating film suggests that MSCG can form a stronger, wear-resistant protective film on the friction surface.[40] This boundary film effectively reduces wear under high loads and maintains a low friction coefficient, significantly enhancing the grease's tribological properties. Conversely, the lubricating film of CSCG, mainly composed of Fe_2O_3 and $CaCO_3$, although offering some degree of hardness and lubricity, is more prone to damage under high loads, leading to inferior tribological performance.

Overbased sulfonates, constituting over 80% of lubricating detergents, also function as the thickener in CSCG. These sulfonates not only clean but also neutralize acidic byproducts from combustion and oxidation in lubricating oils, providing anti-corrosion, anti-rust, and high-pressure properties. The structure of overbased sulfonates features reverse micelles, with hydrophobic groups on the outer layer and hydrophilic groups inside.[9] Acid molecules penetrate these micelles, reacting with the $CaCO_3$ core. Simultaneously, these overbased reverse micelles adsorb at the acid–oil interface. The water absorbed in grease primarily exists as free water, which can disrupt the colloidal structure and degrade performance. This free water

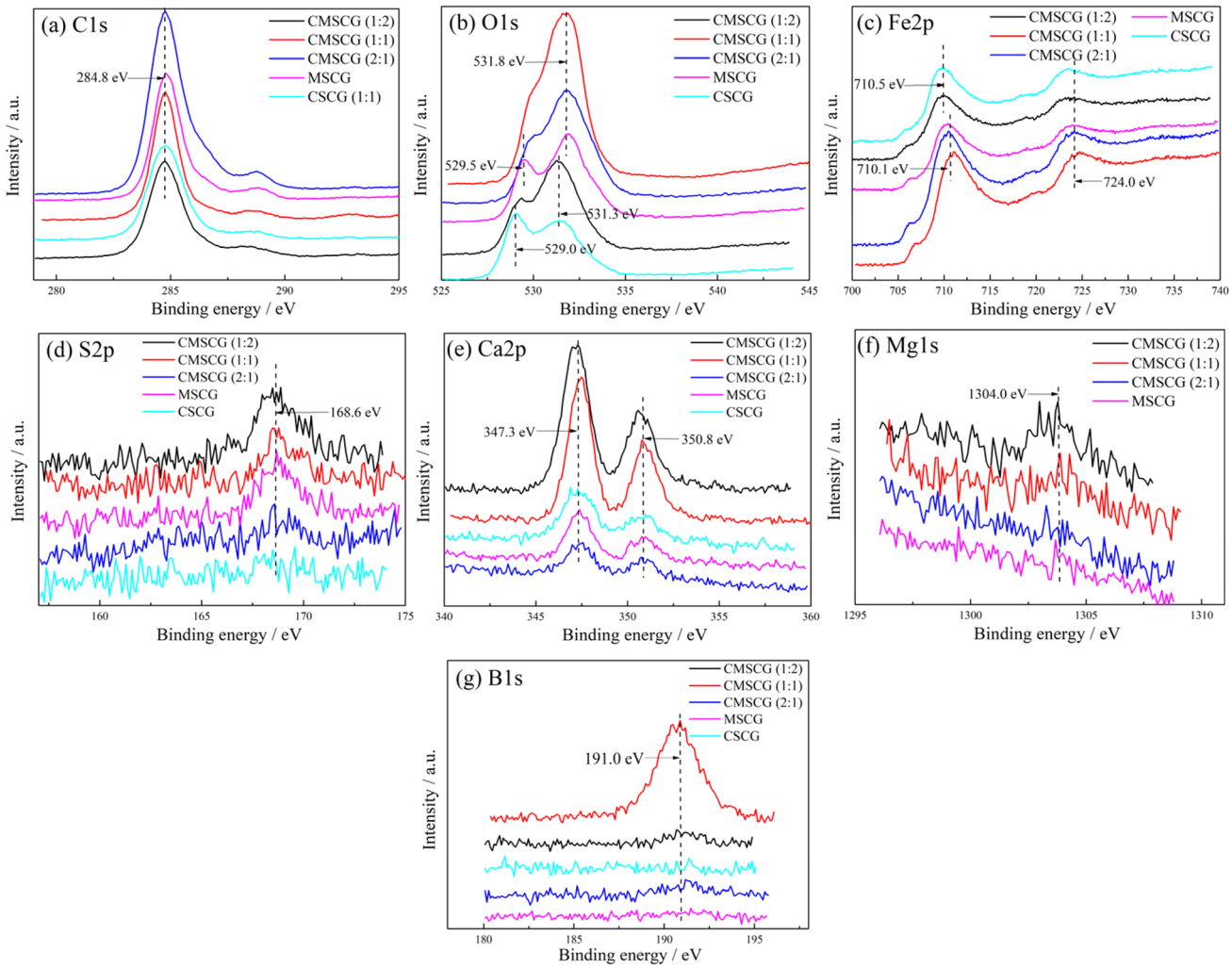

Fig. 12 XPS results of the wear surface lubricated by as-prepared grease, (a) C 1s, (b) O 1s, (c) Fe 2p, (d) S 2p, (e) Ca 2p, (f) Mg 1s, (g) B 1s.

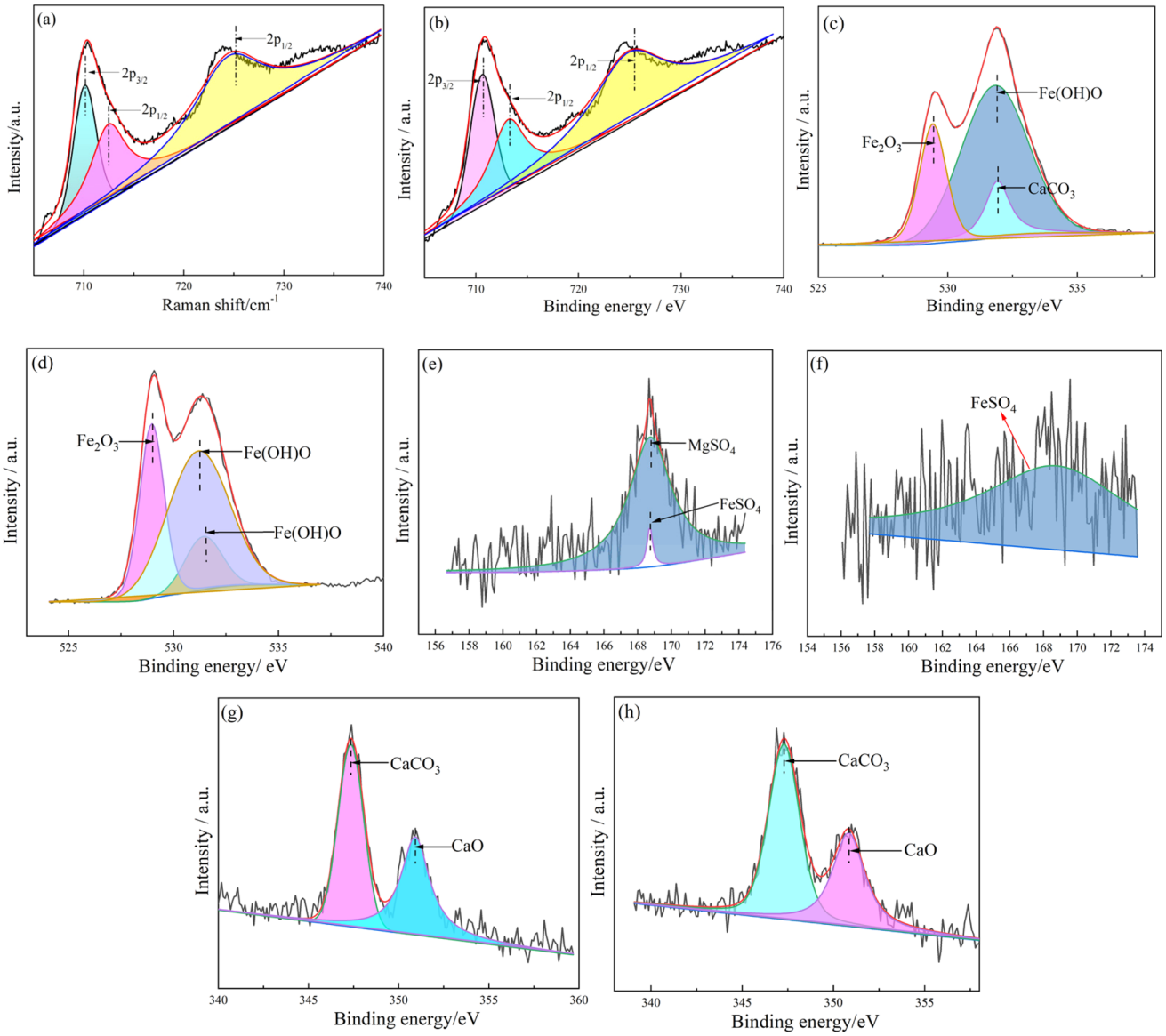

Fig. 13 The deconvoluted XPS spectra of wear scar lubricated by MSCG and CSCG, (a and b) Fe 2p, (c and d) O 1s, (e and f) S 2p, (g and h) Ca 2p.

not only damages the grease's colloidal structure but also acts as a corrosive agent on the matrix surface. The hydrophilic groups of alkyl benzene sulfonate effectively trap most water molecules within the core of the overbased sulfates, limiting their mobility and significantly reducing the amount of free water in the grease. This capacity to absorb water helps maintain the colloidal structure and ensure excellent sealing properties. High-performance detergents like T106D and T107 are characterized by high alkali values, low ash content, water resistance, and superior rust resistance.[41] T107 neutralizes inorganic acids more rapidly than T106D, though it is slower in neutralizing organic acids. Due to the synergistic effects of T106D and T107, the synthesized lubricant demonstrates outstanding corrosion resistance.

In lubricants, sulfonate detergents serve multiple functions, including anti-corrosion, cleaning, friction reduction, and wear resistance. Previous studies attribute the excellent extreme pressure and load-bearing capabilities of overbased detergents to the anti-wear boundary film they form on wear surfaces.[29] Mechanically, overbased sulfonate particles are captured at the contact inlet, adhering to the worn area. Within the T106D's structure, ultrathin calcite layers possess a high surface area, promoting adherence and deposition on metal surfaces. The alkyl benzene sulfonates' polar groups align preferentially, with the *c*-axis standing perpendicular to the $CaCO_3$ surface. Under varying contact pressures, the structure of alkyl benzene sulfonates reacts sensitively; low pressures and shear forces fragment these molecules, while high pressures disrupt ionic bonds between sulfur and calcium, facilitating detachment from the protective film. Initially, overbased sulfonates establish a slender boundary film, which thickens with ongoing friction. Fig. 14 depicts the evolution of this film, which enhances the lubricating oil film and guards the contact surface against wear. XPS findings suggest that T107 formed the tribofilm, correlating

Table 6 The FWHM and area of XPS peaks

Element	Grease	Peak	FWHM	Area
Fe 2p	MSCG	710.1	2.7	33 693
		712.3	4.4	42 916
		724.4	8.5	77 855
	CSCG	710.6	2.8	36 346
		713.1	4.2	44 100
		724.8	8.6	86 825
O 1s	MSCG	529.4	1.2	39 728
		531.8	3.0	109 330
		531.9	1.1	21 247
	CSCG	529.0	1.4	42 997
		531.2	3.5	80 724
		531.4	2.1	18 557
S 2p	MSCG	168.7	3.5	4546
	CSCG	168.8	10.8	6460
Ca 2p	MSCG	347.3	1.7	5010
		350.9	1.9	4587
	CSCG	347.3	2.0	7391
		350.8	2.1	4869

with the inferior anti-wear performance observed in MSCG and CMSCG. The substantial boundary film formed by overbased sulfonates prevents direct contact by strongly adhering to the metal surface, akin to the tribochemical films produced by phosphorus and boron-based additives.[31] As a result, the synergistic effect of T106D and T107 in the formation of tribo-film improves the tribological properties of CSCG.

4 Conclusions

5 Calcium sulfonate complex greases were prepared by different ratio of overbased sulfonates. The synergy effect of overbased sulfonates on physicochemical, anti-corrosion, rheological, and friction-wear performance was investigated. The conclusions were drawn as follows:

(1) The CMSCG (1 : 2) presented the best physicochemical properties (highest dropping point: 354 °C, lowest penetration: 161 (0.1 mm), lowest oil separation: 1.25%), indicating the combination of T106D and T107 in a 1 : 2 ratio shows the excellent compatibility with base oil. The CMSCGs improved the corrosion resistance of calcium sulfonate complex grease, which are attributed to the protective layer formed by overbased sulfonates on metal surfaces.

(2) The MSCG showed highest yield stress (558 Pa), because the flower-like thickener structure provided the high structure strength. In contrast, CSCG shows the lowest yield stress (160 Pa) due to the poor compatibility of T106D with base oil. The hysteresis area of CMSCG (2 : 1) and CSCG were lower than those of other greases due to their excellent thixotropy.

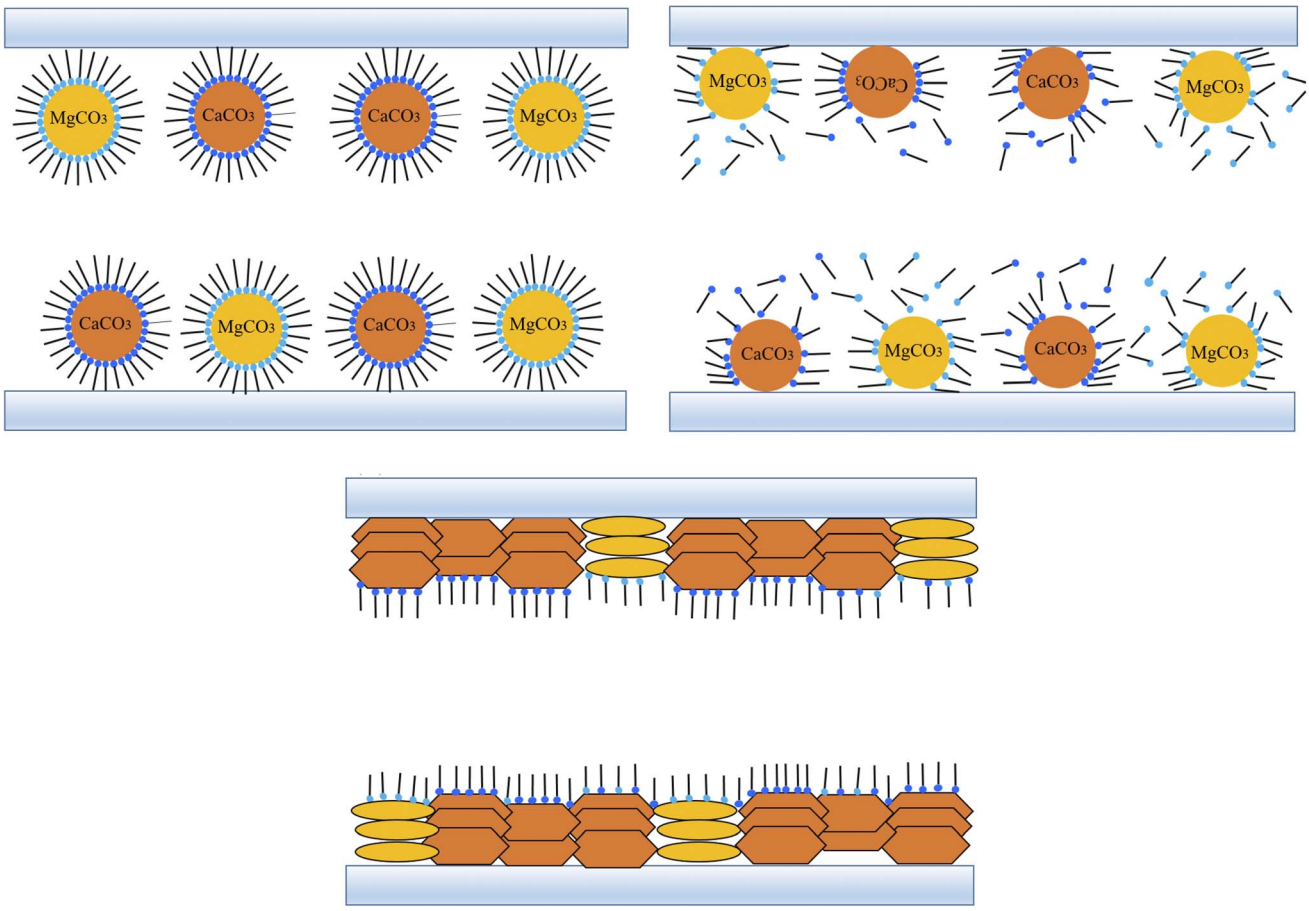

Fig. 14 The evolution of the overbased sulfonates during the friction.

(3) The MSCG presents the optimal friction reduction property and CMSCG (1 : 1) presents the optimal anti-wear property. The friction mechanism indicated that the boundary film formed on the wear surface, including iron oxide, $FeSO_4$, $CaCO_3$, CaO, and $MgCO_3$.

Data availability

The datasets generated during and/or analyzed during the current study are available from the corresponding author on reasonable request. Detailed data supporting the findings of this study, including raw and processed data, are available from the corresponding author, Guanlin Ren, upon reasonable request. This includes experimental results, physicochemical measurements, rheological and tribological test outcomes as detailed within the manuscript.

Author contributions

Ming Zheng: date curation, resources, investigation, and writing – original draft and writing – review & editing. Guanlin Ren: supervision, funding acquisition, and project administration. Siyuan, Wang: methodology and validation. Yulong Li: conceptualization and formal analysis. Mingcai Xing: methodology and formal analysis.

Conflicts of interest

There are no conflicts to declare.

Acknowledgements

The authors gratefully acknowledge the support by the China Scholarship Council program (202306130102) and Postgraduate Scientific Research Innovation Project of Hunan Province (CX20230422).

References

1 M. C. Xing, S. Liu, Y. Cui, J. Q. Xu Z. H. Xu, L. N. Gao, *et al.*, A Comprehensive Sliding Wear Prediction Method for Planetary Roller Screw Mechanism, *Wear*, 2024, **558**, 205536, DOI: **10.1016/j.wear.2024.205536**.

2 X. Shen, D. J. Yuan, L. Q. Cao, D. L. Jin, X. S. Chen and Z. F. Gao, Experimental investigation of the failure of shield grease seals under the influence of environmental factors: A T106D study, *Eng. Failure Anal.*, 2021, **133**, 105975, DOI: **10.1016/j.engfailanal.2021.105975**.

3 Z. Y. Wang, Y. Q. Xia and Z. L. Liu, The rheological and tribological properties of calcium sulfonate complex greases, *Friction*, 2014, **3**(1), 28–35, DOI: **10.1007/s40544-014-0063-1**.

4 P. Cann, Grease lubrication of rolling element bearings-role of the grease thickener, *Lubr. Sci.*, 2007, **19**(3), 183–196, DOI: **10.1002/ls.39**.

5 H. D. Wang, Y. Wang, Y. H. Liu, J. Zhao, J. J. Li, Q. Wang and J. B. Luo, Tribological behavior of layered double hydroxides with various chemical compositions and morphologies as grease additives, *Friction*, 2021, **9**(5), 952–962, DOI: **10.1007/s40544-020-0380-5**.

6 Z. C. Chen, S. Xiao, F. Chen, D. Z. Chen, J. L. Fang and M. Zhao, Calcium carbonate phase transformations during the carbonation reaction of calcium heavy alkylbenzene sulfonate overbased nanodetergents preparation, *J. Colloid Interface Sci.*, 2011, **359**, 56–67, DOI: **10.1016/j.jcis.2011.03.086**.

7 F. Frigerio, and L. Montanari, Characterisation of the surfactant shell stabilising calcium carbonate dispersions in overbased detergent additives molecular modelling and spin-probe-esr studies, *7th International Conference on Computational Science*, Berlin, Heidelberg, 2007, pp. 272–279.

8 Z. C. Chen, F. Chen and D. Z. Chen, Universal phase transformation mechanism and substituted alkyl length and number effect for the preparation of overbased detergents based on calcium alkylbenzene sulfonates, *Ind. Eng. Chem. Res.*, 2013, **52**(36), 12748–12762, DOI: **10.1021/ie401415s**.

9 M. Najman, M. Kasraia, G. Michael Bancrofta and R. Davidson, Combination of ashless antiwear additives with metallic detergents: interactions with neutral and overbased calcium sulfonates, *Tribol. Int.*, 2006, **39**(4), 342–355, DOI: **10.1016/j.triboint.2005.02.014**.

10 R. Bosman and P. M. Lugt, The microstructure of calcium sulfonate complex lubricating grease and its change in the presence of water, *Tribol. Trans.*, 2018, **61**(5), 842–849, DOI: **10.1080/10402004.2018.1431752**.

11 F. Cyriac, P. M. Lugt and R. Bosman, Impact of water on the rheology of lubricating greases, *Tribol. Trans.*, 2016, **59**(4), 679–689, DOI: **10.1080/10402004.2015.1107929**.

12 T. Kubo, S. Fujiwara, H. Nanao, I. Minami and S. Mori, Boundary film formation from overbased calcium sulphonate additives during the running-in process of steel-DLC contact, *Wear*, 2008, **265**, 461–467, DOI: **10.1016/j.wear.2007.11.027**.

13 K. Topolovec-Miklozic, T. R. Forbus and H. Spikes, Film forming and friction properties of overbased calcium sulphonate detergents, *Tribol. Lett.*, 2008, **29**, 33–44, DOI: **10.1007/s11249-007-9279-9**.

14 E. V. Kobylyansky, O. A. Mishchuk and Yu. L. Ishchuk, Lubricating properties of thixotropic systems based on overbased calcium sulphonate, *Lubr. Sci.*, 2004, **16**(3), 293–302, DOI: **10.1002/ls.3010160308**.

15 F. Chinas-Castillo and H. Spikes, Film formation by colloidal overbased detergents in lubricated contacts, *Tribol. Trans.*, 2008, **43**(3), 357–366, DOI: **10.1080/0402000008982351**.

16 D. B. Liu, M. Zhang, G. Q. Zhao and X. B. Wang, Tribological behavior of amorphous and crystalline overbased calcium sulfonate as additives in lithium complex grease, *Tribol. Lett.*, 2011, **45**(2), 265–273, DOI: **10.1007/s11249-011-9884-5**.

17 L. Cizaire, J. M. Martin, E. Gresser, *et al.*, Tribochemistry of overbased calcium detergents studied by ToF-SIMS and other surface analyses, *Tribol. Lett.*, 2004, **17**, 715–721, DOI: **10.1007/s11249-004-8078-9**.

18 M. T. Costello, Study of surface films of amorphous and crystalline overbased calcium sulfonate by XPS and AES, *Tribol. Trans.*, 2006, **49**(4), 592–597, DOI: **10.1080/10402000600927563**.

19 M. T. Costello, R. A. Urrego and M. Kasrai, Study of surface films of crystalline and amorphous overbased sulfonates and sulfurized olefins by X-ray absorption near edge structure (XANES) spectroscopy, *Tribol. Lett.*, 2007, **26**, 173–180, DOI: **10.1007/s11249-006-9190-9**.

20 T. Palermo, S. Giasson, T. Buffeteau, *et al.*, Study of deposit and friction films of overbased calcium sulphonate by PM-IRRAS spectroscopy, *Lubr. Sci.*, 1996, **8**(2), 119–127, DOI: **10.1002/ls.3010080203**.

21 A. Greenall, A. Neville, A. Morina, *et al.*, Investigation of the interactions between a novel, organic anti-wear additive, ZDDP and overbased calcium sulphonate, *Tribol. Int.*, 2012, **46**(1), 52–61, DOI: **10.1016/j.triboint.2011.06.016**.

22 C. J. Zhou, G. L. Ren, X. Q. Fan and Y. Y. Lv, Probing the effect of thickener microstructure on rheological and tribological properties of grease, *J. Ind. Eng. Chem.*, 2022, **111**, 51–63, DOI: **10.1016/j.jiec.2022.03.010**.

23 J. Tan, Y. Wang, M. Liu, *et al.*, Study of the effect of overbased calcium or magnesium sulfonate combinated with thiazole derivatives in rapeseed oil on tribological properties, *Ind. Lubr. Tribol.*, 2018, **70**(7), 1258–1267, DOI: **10.1108/ILT-10-2017-0314**.

24 C. H. Xiong, H. Y. Mi, Q. Feng and B. J. Wu, Comparative studies on low noise greases operating under high temperature oxidation condition, *China Pet. Process. Petrochem. Technol.*, 2014, **16**(4), 100–106, **https://api.semanticscholar.org/CorpusID:136773975**.

25 J. W. Tavacoli, P. J. Dowding, D. C. Steytler, D. J. Barnes and A. F. Routh, Effect of water on overbased sulfonate engine oil additives, *Langmuir*, 2008, **24**, 3807–3813, DOI: **10.1021/la703680e**.

26 S. Liu, Y. Jing, T. T. Zhang, J. Zhang, F. Xu, Q. Song, Q. Ye, S. J. Liu and W. M. Liu, Excellent tribological and anti-corrosion performances enabled by novel hollow graphite carbon nanosphere with controlled release of corrosion inhibitor, *Chem. Eng. J.*, 2021, **412**, 128648, DOI: **10.1016/j.cej.2021.128648**.

27 Y. X. Zhou, R. Bosman and P. Lugt, On the shear stability of dry and water-contaminated calcium sulfonate complex lubricating greases, *Tribol. Trans.*, 2019, **62**(4), 626–634, DOI: **10.1080/10402004.2019.1588445**.

28 S. K. Yeong, P. F. Luckham and Th. F. Tadros, Steady flow and viscoelastic properties of lubricating grease containing various thickener concentrations, *J. Colloid Interface Sci.*, 2004, **274**(1), 285–293, DOI: **10.1016/j.jcis.2004.02.054**.

29 W. Lisowski, A. H. J. Van Den Berg, M. Smither and V. A. C. Haanappel, Characterization of thin alumina films prepared by metal-organic chemical vapour deposition (mocvd) by high resolution SEM, (AR)XPS and AES depth profiling, *Fresenius. J. Anal. Chem.*, 1995, **353**(5–8), 707–712, DOI: **10.1007/BF00321355**.

30 X. B. Ji, Y. X. Chen, G. Q. Zhao, X. B. Wang and W. M. Liu, Tribological properties of $CaCO_3$ nanoparticles as an additive in lithium grease, *Tribol. Lett.*, 2011, **41**(1), 113–119, DOI: **10.1007/s11249-010-9688-z**.

31 C. X. Zhang, Z. Q. Song, Z. F. Liu, Q. Cheng, Y. S. Zhao, C. B. Yang and M. M. Liu, Wear mechanism of flexspline materials regulated by novel amorphous/crystalline oxide form evolution at frictional interface, *Tribol. Int.*, 2019, **135**, 335–343, DOI: **10.1016/j.triboint.2019.03.023**.

32 L. L. Zhu, X. H. Wu, G. Q. Zhao and X. B. Wang, Tribological characteristics of bisphenol af bis(diphenyl phosphate) as an antiwear additive in polyalkylene glycol and polyurea grease for significantly improved lubrication, *Appl. Surf. Sci.*, 2016, **363**, 145–153, DOI: **10.1016/j.apsusc.2015.12.008**.

33 W. Wang, S. H. Qian, L. F. Gong, Z. F. Ni and H. D. Ren, Effects of carbon nano onions on the tribological performance of food-grade calcium sulfonate complex grease, *Lubr. Sci.*, 2021, **33**(8), 460–470, DOI: **10.1002/ls.1567**.

34 M. J. G. Guimarey, J. M. Liñeira Del Rio and J. Fernández, Improvement of the lubrication properties of grease with Mn_3O_4_graphene (Mn_3O_4) nanocomposite additive, *J. Mol. Liq.*, 2022, **350**, 118550, DOI: **10.1007/s40544-020-0412-1**.

35 D. Y. Zhang, Z. W. Li, X. Wei, L. P. Wang, J. B. Xu and Y. F. Liu, Study tribological properties of MoDTC and its interactions with metal detergents, *J. Tribol.*, 2020, **142**(12), 122201, DOI: **10.1115/1.4047457**.

36 B. Jin, G. Y. Chen, J. Zhao, Y. Y. He, Y. Y. Huang and J. B. Luo, Improvement of the lubrication properties of grease with Mn_3O_4/graphene (Mn_3O_4#G) nanocomposite additive, *Friction*, 2021, **9**(6), 1361–1377, DOI: **10.1007/s40544-020-0412-1**.

37 N. Li, S. Guo, B. Pan, M. Xie, J. Yan and Z. Chen, The Effect of 1T Phase Molybdenum Disulfide on the Tribological Performance of Polyethylene Glycol, *J. Tribol.*, 2022, **44**, 2124748, DOI: **10.1080/00222348.2022.2124748**.

38 M. Xie, B. Pan, N. Li, S. Zhao, J. Yan, S. Guo, Z. Chen and H. Wang, 2D graphene/FeOCl heterojunctions with enhanced tribology performance as a lubricant additive for liquid paraffin, *RSC Adv.*, 2022, **11**, 6650–6660, DOI: **10.1039/d1ra06650a**.

39 S. Xiang, X. Zhi, H. Bao, Y. He, Q. Zhang, S. Lin, B. Hu, S. Wang, P. Lu, X. Yang, Q. Tian and X. Du, Tribological Behavior of GTL Base Oil Improved by Ni-Fe Layered Double Hydroxide Nanosheets, *Lubricants*, 2024, **12**, 146, DOI: **10.3390/lubricants12050146**.

40 W. Chen, K. Thummavichai, X. Chen, G. Liu, X. Lv, L. Zhang, D. Chen, S. K. Tiwari, N. Wang and Y. Zhu, Design and Evaluation the Anti-Wear Property of Inorganic Fullerene Tungsten Disulfide as Additive in PAO6 Oil, *Crystals*, 2021, **11**, 570, DOI: **10.3390/CRYST11050570**.

41 S. Y. Wang, G. L. Ren, W. Q. Li, B. Wang, F. H. Wei, Z. Liang and D. Chen, A green modification technology of carbon nanotubes toward enhancing the tribological properties of aqueous-based lubricants, *Tribol. Int.*, 2023, **180**, 108268, DOI: **10.1016/j.triboint.2023.108268**.